EJMI

DOI: 10.14744/ejmi.269449
EJMI 2026;10(3):449–457


Research Article

# Integrating Quantitative CT Metrics with Biochemical Profiles in the Assessment of Steatotic Liver Disease

**Abdullah Enes Ataş,**[1] **Hasan Emin Kaya**[2]

[1]Department of Radiology, Necmettin Erbakan University, School of Medicine, Konya, Türkiye
[2]Department of Radiology, Bursa Uludağ University School of Medicine, Bursa, Türkiye

**Abstract**

**Objectives:** This study aimed to evaluate the utility of quantitative CT metrics in assessing metabolic liver injury by integrating radiological findings with biochemical profiles and non-invasive fibrosis scores.

**Methods:** We retrospectively analyzed 225 patients who underwent unenhanced abdominal CT. Liver attenuation (HU), liver-to-spleen (L/S) ratio, liver-spleen difference (L-S diff), and subcutaneous fat thickness (SFT) were measured and correlated with serum transaminases, gamma-glutamyl transferase (GGT), and FIB-4 scores.

**Results:** While absolute liver density (<40 HU) identified steatosis in 9.3% of the cohort, the L-S difference (<10 HU) expanded detection to 56.8%. GGT demonstrated the strongest inverse correlation with absolute liver density (p=0.005) and was the most robust biochemical predictor in ROC analysis (AUC=0.669); the liver-spleen difference showed similar performance (AUC=0.663, p=0.008). The L-S difference was the sole parameter associated with significant elevations in AST, ALT, and GGT simultaneously. Radiologically defined steatosis correlated with higher FIB-4 scores (p<0.05), whereas no correlation was observed with APRI scores.

**Conclusion:** Quantitative unenhanced CT parameters, particularly the liver-spleen attenuation difference, correlate significantly with GGT levels and FIB-4 scores. These accessible metrics serve as valuable tools for the opportunistic screening of steatotic liver disease, reflecting both morphological changes and underlying metabolic dysfunction beyond simple fat accumulation.

**Keywords:** Adiposity, Biomarkers, Gamma-glutamyltransferase, Non-alcoholic Fatty liver disease, Tomography, X-ray computed

***Cite This Article:*** *Ataş AE, Kaya HE. Integrating Quantitative CT Metrics with Biochemical Profiles in the Assessment of Steatotic Liver Disease. EJMI 2026;10(3):449–457.*

Metabolic dysfunction-associated steatotic liver disease (MASLD) represents a dynamic clinical spectrum rather than a static condition. This spectrum extends from simple, benign steatosis to metabolic dysfunction-associated steatohepatitis (MASH), a state characterized by active inflammation, progressive fibrosis, and the potential for cirrhosis or hepatocellular carcinoma.[1] With a global prevalence nearing 30%, the burden of MASLD is not limited to hepatic pathology; it is increasingly recognized as an independent driver of diabetes and cardiovascular morbidity.[2]

While liver biopsy is historically the reference standard for definitive diagnosis and staging, it is largely impractical for routine screening or longitudinal monitoring. Its invasive nature, associated costs, procedural risks such as hemorrhage, and the potential for sampling error due to hetero-

**Address for correspondence:** Abdullah Enes Ataş, MD, Department of Radiology, Necmettin Erbakan University, School of Medicine, Konya, Türkiye
**Phone:** +90 555 680 18 09 **E-mail:** aenesatas@gmail.com

**Submitted Date:** June 4, 2026 **Revised Date:** August 5, 2026 **Accepted Date:** August 19, 2026

geneous parenchymal involvement limit its widespread utility. These constraints have shifted clinical focus toward non-invasive imaging modalities, making abdominal ultrasonography (US) and computed tomography (CT) essential tools for steatosis detection.[3]

In this landscape, unenhanced abdominal CT scans obtained for non-hepatic indications, such as renal colic, trauma, or non-specific abdominal pain, provide a valuable avenue for opportunistic screening.[4] These examinations allow for the objective assessment of liver parenchymal metabolism without subjecting the patient to additional radiation exposure or financial cost.[5] Existing literature consistently demonstrates a robust inverse correlation between liver parenchymal density (measured in Hounsfield units) and the histopathological grade of steatosis. Conventionally, an absolute liver attenuation value below 40 HU or a liver-to-spleen (L/S) attenuation ratio of <1.0 is accepted as diagnostic for steatosis.[6]

Recent evidence, however, suggests that these static thresholds lack universality. Factors such as age-related parenchymal changes, sex-hormone profiles, and anemia can confound density measurements. Consequently, strict adherence to traditional cut-off values may be insufficient for capturing early-stage metabolic alterations, leaving a diagnostic 'gray zone'.[7]

In routine clinical practice, biochemical surveillance of hepatic steatosis centers on alanine aminotransferase (ALT) and aspartate aminotransferase (AST) as surrogate markers of hepatocellular injury.[8] Yet, a reliance on these enzymes alone can be misleading; a substantial subset of patients maintains aminotransferase levels within laboratory reference ranges despite having histologically proven steatosis or advanced fibrosis.[9] This phenotype, often described as 'MASLD with normal ALT', masks the silent progression of the disease and highlights the urgent need for biomarkers sensitive enough to detect subclinical injury.[10]

Against this background, gamma-glutamyl transferase (GGT) is gaining recognition beyond its traditional role as an indicator of alcohol consumption. It is increasingly viewed as an early sentinel for oxidative stress, the depletion of cellular antioxidants (specifically glutathione), and insulin resistance.[11] Parallel to this, the AST/ALT ratio (De Ritis ratio) offers distinct prognostic value in assessing fibrosis and metabolic risk, differentiating metabolic liver pathologies from viral hepatitis.[12]

While prior studies have largely examined absolute liver attenuation or the L/S ratio in isolation, and typically in relation to a single biochemical marker such as ALT, the present study distinguishes itself by simultaneously evaluating three complementary quantitative CT indices—absolute liver density, L/S ratio, and L-S difference—against a broader biochemical panel encompassing GGT, the AST/ALT ratio, and two independent non-invasive fibrosis scores (FIB-4 and APRI). This multi-parametric approach allows direct comparison of the relative diagnostic contribution of each radiological metric, an aspect that remains underexplored in the current literature.

This study aims to evaluate the association between quantitative radiological measurements and clinical biochemical profiles to identify potential non-invasive markers for opportunistic screening. By investigating the relationship between parameters derived from liver density on unenhanced CT and early markers of metabolic dysfunction and oxidative stress, it aims to assess the predictive potential of these metrics for opportunistic risk stratification in an asymptomatic population.

## Methods

### Study Population and Design

This retrospective, cross-sectional study was conducted following approval by the Necmettin Erbakan University Non-Pharmaceutical and Non-Medical Device Research Ethics Committee (Decision Date: 12 December 2025; Approval No.: 2025-6199). We screened patients over 18 years of age who underwent unenhanced abdominal CT for various indications (e.g., suspected renal colic, trauma screening, non-specific abdominal pain) at a tertiary care center between 1 January 2024 and 1 January 2025.

In accordance with the multi-society consensus nomenclature statement, MASLD was defined as the presence of radiologically confirmed hepatic steatosis (determined by unenhanced CT metrics) in combination with at least one of the established cardiometabolic risk factors (such as type 2 diabetes mellitus, hyperlipidemia, or systemic hypertension), which were verified through institutional ICD-10 diagnosis codes and electronic medical prescription records.

Because this study aimed to evaluate different quantitative CT thresholds, radiological steatosis was dynamically assessed using three different criteria (absolute liver density <40 HU, L/S ratio <1.0, and L-S difference <10 HU) to observe how each metric affects the diagnostic yield of MASLD within the cohort.

Strict exclusion criteria were defined to ensure a clear association between radiological data and biochemical parameters. Patients were excluded if they had:

- Known chronic liver disease (viral hepatitis B or C, autoimmune hepatitis, hemochromatosis),
- A history of hepatotoxic drug use affecting liver density (e.g., amiodarone, tamoxifen, methotrexate),

- Active malignancy or recent chemotherapy,
- A history of significant alcohol consumption.

Initially, a total of 447 patients who underwent unenhanced abdominal CT were screened. Of these, 39 patients were excluded due to known chronic liver diseases, 56 patients due to a history of hepatotoxic drug use or active malignancy, 6 patients due to significant alcohol consumption, and 121 patients due to missing concurrent laboratory data within the specified ±24-hour window. Ultimately, a general cohort of 225 patients meeting the eligibility criteria was included in the final analysis to evaluate the prevalence and biochemical correlates of steatosis.

## Radiological Assessment

CT examinations were performed using a 256-detector CT scanner (Siemens Somatom, Erlangen, Germany) in accordance with standard protocols. Since attenuation values are dependent on tube voltage, a standard 120 kVp tube voltage and automatic tube current modulation were used for all recordings. All CT examinations were obtained without the injection of contrast agent. Images were analyzed on a workstation integrated into the hospital information system by a radiologist with 10 years of experience in abdominal radiology, blinded to the patients' clinical information. To evaluate inter-observer reliability, a randomly selected subset of patients (n=40) was independently re-evaluated by a second radiologist with 12 years of experience, who was also blinded to the clinical data. The intraclass correlation coefficient (ICC) was calculated using a two-way mixed-effects model to assess the reproducibility of the attenuation measurements.

To ensure measurement standardization, liver parenchymal density (HU) was calculated by averaging three circular areas of interest (ROI) measurements, each covering an area of 150–200 $mm^2$, taken from the anterior and posterior segments of the right lobe and the lateral segments of the left lobe; this process carefully avoided large vascular structures, bile ducts, calcifications, and artifacts (Fig. 1). Splenic parenchymal density was measured using a similar method to serve as the patient's internal reference. Using these data, the liver/spleen (L/S) ratio and liver-spleen (L-S) difference were calculated. As an indicator of visceral adiposity, subcutaneous fat tissue thickness (SFT) was measured at the umbilical level along the midline.

## Biochemical and Clinical Parameters

Serum ALT, AST, GGT, and platelet levels, obtained from fasting blood samples collected concurrently with the CT scan (maximum interval of ±24 hours), were retrospectively recorded from the hospital laboratory information system. To non-invasively exclude the risk of liver fibrosis and ensure the homogeneity of the study cohort, the AST/ALT ratio, FIB-4 index [(Age × AST) / (Platelets × √ALT)], and APRI score [(AST / Upper Limit of Normal) × 100 / Platelets] were calculated.[12-14] The presence of diabetes and hyperlipidemia was verified via ICD diagnosis codes and prescription records in the patients' medical history.

Cases with missing concurrent laboratory data within the specified ±24-hour window were excluded from the analysis using listwise deletion.

## Statistical Analysis

Data analysis was performed using SPSS v24.0 (IBM Corp., Armonk, NY) and Jamovi v2.6 (Sydney, Australia). The normality of variable distribution was assessed using the Kolmogorov-Smirnov test and histogram analyses. Intergroup comparisons were conducted using the independent-samples t-test or Mann-Whitney U test, depending on distribution characteristics. To determine the direction and strength of relationships between variables, Pearson correlation coefficients were calculated. Multivariate linear regression analyses were applied to identify independent predictors and eliminate confounding factors. Furthermore, receiver operating characteristic (ROC) curve analysis was performed to evaluate the discriminatory capability of radiological parameters. A two-tailed p-value of <0.05 was initially considered statistically significant. However, to control for the inflated risk of Type I errors associated with multiple comparisons in our correlation analyses, the Benjamini-Hochberg procedure was applied to control the false discovery rate (FDR). An FDR threshold of 0.05 was maintained to ensure the robustness of the significant correlations without excessively sacrificing statistical power.

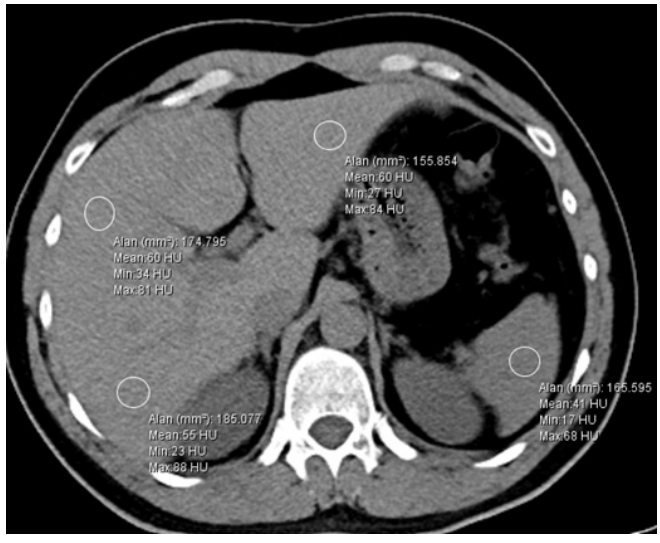


**Figure 1.** Representative unenhanced CT image showing the placement of regions of interest (ROIs) for the assessment of liver and spleen attenuation values (Hounsfield Unit).

## Results

A total of 225 patients (mean age: 49.6±13.7 years; 50.2% male) were included in the study. The prevalence of diabetes and hyperlipidemia was found to be 21.7% and 24.8%, respectively. The mean liver density was 55.0±10.1 HU, with the wide standard deviation indicating significant population heterogeneity regarding liver steatosis. Detailed demographic and radiological data are summarized in Table 1.

### Radiological Steatosis

When the L/S ratio <1.0 criterion was applied for the radiological diagnosis of steatosis, hepatic steatosis was identified in 39 of the 225 patients (17.3%). Conversely, when the criterion of absolute liver density <40 HU was utilized, the prevalence was found to be 9.3% (n=21). This specific subgroup is considered to represent 'moderate-to-severe steatosis,' corresponding to a liver fat content exceeding 30%. Additionally, using the L-S difference <10 HU criterion, steatosis was detected in 128 patients (56.8%).

Inter-observer reliability analysis demonstrated excellent agreement between the two radiologists for the quantitative CT measurements, yielding an intraclass correlation coefficient (ICC) of 0.91.

### Correlation Analysis Between Radiological and Biochemical Parameters

A correlation analysis was conducted to evaluate the relationship between quantitative CT parameters (liver density, L/S ratio, L-S difference) and metabolic/biochemical markers. Correlations were assessed using the Pearson correlation coefficient (r). As detailed in Table 2, all three radiological indices demonstrated statistically significant correlations with key liver enzymes and fibrosis scores, with the exception of the APRI score.

**Table 1.** Demographic, radiological, and laboratory characteristics of the study group.

| Parameter | Mean±SD |
|---|---|
| Age (years) | 49.6±13.7 |
| Diabetes mellitus | 49 (21.7%) |
| Hyperlipidemia | 56 (24.8%) |
| Liver Density (HU) | 55.0±10.1 |
| Spleen Density (HU) | 47.3±2.7 |
| L/S Ratio | 1.15±0.16 |
| L-S Difference (HU) | 7.6±7.9 |
| Subcutaneous Fat Thickness (mm) | 21.4±7.2 |
| ALT (U/L) | 25.2±11.5 |
| AST (U/L) | 22.3±7.6 |
| GGT (U/L) | 31.8±17.0 |
| Platelets ($10^9$/L) | 226.2±49.4 |
| De Ritis Ratio (AST/ALT) | 0.97±0.24 |
| FIB-4 Index | 1.08±0.51 |

A consistent negative correlation was observed between liver density parameters and serum transaminases, indicating that as liver density decreases (indicating increasing steatosis), enzyme levels rise. GGT exhibited the strongest correlation among the enzymatic markers, particularly with absolute liver density (r=-0.266, p=0.005) and the L/S ratio (r=-0.211, p=0.001). ALT levels also showed a significant negative correlation with liver density (r=-0.239, p=0.029) and L/S ratio (r=-0.199, p=0.002). AST demonstrated a similar, albeit slightly weaker, inverse relationship with all three radiological parameters (p<0.05).

A significant positive correlation was identified between the AST/ALT ratio and radiological parameters (liver density: r=0.182, p=0.006; L/S ratio: r=0.158, p=0.029).

**Table 2.** Correlation coefficients (r) and significance levels (p) describing the relationship between CT density measurements and clinical laboratory values

| Parameter | Liver density (HU) | L/S ratio | L-S difference |
|---|---|---|---|
| AST (U/L) | p=0.02 (r= -0.153) | p=0.04 (r= -0.132) | p=0.05 (r= -0.13) |
| ALT (U/L) | p=0.029 (r= -0.239) | p=0.002 (r= -0.199) | p=0.002 (r= -0.2) |
| GGT (U/L) | p=0.005 (r= -0.266) | p=0.001 (r= -0.211) | p=0.007 (r= -0.223) |
| PLT ($10^9$/L) | p=0.019 (r= 0.156) | p=0.01 (r= 0.171) | p=0.01 (r= 0.168) |
| AST/ALT Ratio | p=0.006 (r= 0.182) | p=0.029 (r= 0.158) | p=0.022 (r= 0.152) |
| FIB-4 Index | p=0.001 (r= -0.211) | p=0.003 (r= -0.234) | p=0.005 (r= -0.23) |
| APRI | p=0.68 | p=0.88 | p=0.89 |
| Subcutaneous Fat Thickness (mm) | p=0.001 (r= -0.248) | p<0.001 (r= -0.301) | p<0.001 (r= -0.298) |

HU: Hounsfield unit; L/S: Liver-to-spleen; AST: Aspartate aminotransferase; ALT: Alanine aminotransferase; GGT: Gamma-glutamyl transferase; PLT: Platelet count; FIB-4: Fibrosis-4 ındex; APRI: AST to platelet ratio ındex.

This finding implies that as liver density decreases due to fat accumulation, the AST/ALT ratio also tends to decrease (shifting toward <1.0), which is consistent with the metabolic steatosis phenotype. Platelet counts (PLT) showed a significant positive correlation with liver density (r=0.156, p=0.019) and L/S ratio (r=0.171, p=0.01), suggesting that lower platelet counts are associated with lower liver density.

The FIB-4 index demonstrated a significant inverse correlation with liver density (r=-0.211, p=0.001) and L/S ratio (r=-0.234, p=0.003), indicating that radiologically detected steatosis is associated with higher FIB-4 values. In contrast, the APRI score did not show a statistically significant correlation with any of the radiological parameters (p>0.05).

Patients were stratified based on three quantitative CT parameters in Table 3: absolute liver density (≤40 HU vs. >40 HU), liver-to-spleen (L/S) ratio (<1 vs. ≥1), and liver-spleen attenuation difference (<10 HU vs. ≥10 HU).

When grouped by absolute liver density, patients with steatosis (≤40 HU) demonstrated significantly higher FIB-4 scores compared to the non-steatotic group (1.60±0.96 vs. 1.04±0.51; p=0.005) and increased subcutaneous fat thickness (SFT) (p=0.001). However, no statistically significant difference was observed in liver enzyme levels (AST, ALT, GGT) between these groups.

Similarly, in the analysis based on the L/S ratio, the group indicative of steatosis (<1) showed significantly higher FIB-4 scores (p=0.03) and lower platelet counts (p=0.02) compared to the group with an L/S ratio ≥1.

Notably, the liver-spleen attenuation difference was the only parameter that revealed significant differences across all liver enzymes. Patients with a difference of <10 HU had significantly higher levels of ALT (p=0.03), AST (p=0.01), and GGT (p=0.002) compared to those with a difference ≥10 HU. Subcutaneous fat thickness was consistently higher in the steatotic groups across all three classification methods (p<0.01 for all).

Multivariate linear regression analysis revealed that the model significantly predicted the AST/ALT ratio (F-test p=0.01, adjusted $R^2$=0.19) (Table 4). GGT levels (β=-0.40, p<0.001) and male gender (β=-0.26, p=0.02) were identified as significant independent predictors inversely correlated with the ratio. Diabetes mellitus showed a borderline positive correlation (p=0.05). No significant association was observed between the AST/ALT ratio and radiological parameters, including liver density (p=0.07) and subcutaneous fat thickness (p=0.51).

Receiver operating characteristic (ROC) curve analysis was performed to evaluate the discriminatory capability of quantitative CT parameters in predicting an AST/ALT (De Ritis) ratio of <1 (Fig. 2). The analysis revealed that none of the unenhanced CT indices demonstrated significant diagnostic accuracy for this specific biochemical threshold. The area under the curve (AUC) values for absolute liver density (AUC=0.549; 95% CI: 0.468–0.630; p=0.23), liver-to-spleen ratio (AUC=0.545; 95% CI: 0.465–0.626; p=0.27), and liver-spleen difference (AUC=0.546; 95% CI: 0.465–0.626; p=0.26) were all close to 0.5, indicating no discriminative power for predicting an inverted AST/ALT ratio in this cohort.

ROC curve analysis was performed to determine the discriminatory capability of unenhanced CT parameters in predicting elevated serum GGT levels (>50 U/L) (Fig. 3) (Table 5). Absolute liver density (HU) yielded the highest discriminatory capability, with an AUC of 0.669 (95% CI: 0.550–0.789; p=0.005). To balance clinical utility for oppor-

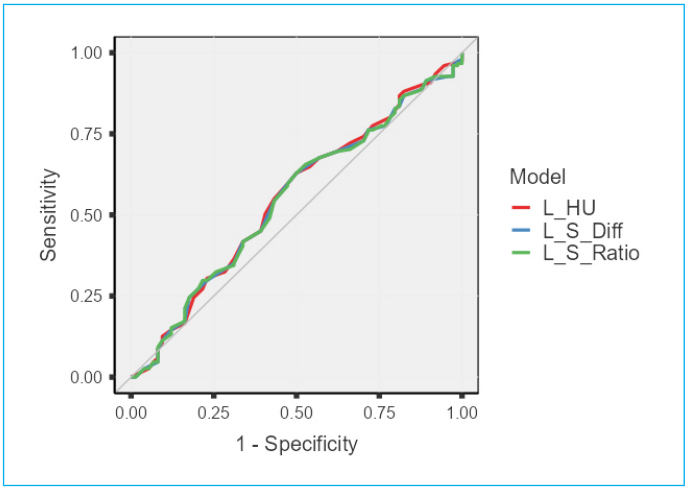


**Figure 2.** ROC curves illustrating the predictive potential of liver density (L_HU), liver-to-spleen difference (L_S_Diff), and liver-to-spleen ratio (L_S_Ratio) in predicting an AST/ALT ratio <1.

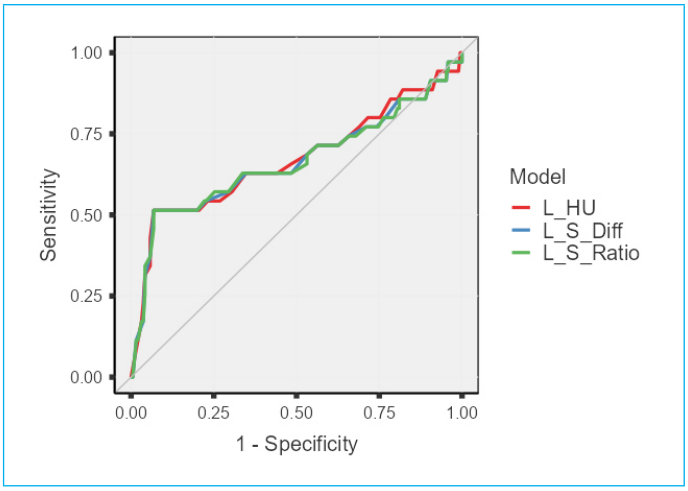


**Figure 3.** ROC curves illustrating the performance of quantitative CT indices for the prediction of elevated GGT (>50 U/L).

**Table 3.** Comparison of biochemical markers, fibrosis scores according to liver attenuation thresholds on unenhanced CT

| Parameter | Liver density | | p | Liver/Spleen ratio | | p | Liver-Spleen difference | | p |
|---|---|---|---|---|---|---|---|---|---|
| | <40 HU (n=21) | >40 HU (n=204) | | <1 (n=39) | ≥1 (n=186) | | <10 (n=97) | ≥10 (n=128) | |
| ALT (U/L) | 25.4±11.1 | 23.5±15.3 | 0.48 | 22.2±13.7 | 25.8±10.9 | 0.13 | 27.8± 11.9 | 23.3±10.9 | 0.03 |
| AST (U/L) | 22.3±7.5 | 22.3±8.5 | 0.96 | 20.7±8.1 | 22.6±7.4 | 0.16 | 23.8±7.3 | 21.2±7.6 | 0.01 |
| GGT (U/L) | 32.2±19.7 | 31.5±16.8 | 0.84 | 32.2±16.9 | 29.5±17.7 | 0.41 | 37.0±17.2 | 27.4±15.7 | 0.002 |
| PLT ($10^3$/uL) | 205±53 | 225±48 | 0.05 | 210±54 | 229±47 | 0.02 | 219.5±47.7 | 235.1±50.4 | 0.01 |
| FIB-4 score | 1.60±0.96 | 1.04±0.51 | 0.005 | 1.36±0.83 | 1.04±0.51 | 0.03 | 1.15±0.63 | 1.02±0.53 | 0.11 |
| APRI | 0.29±0.14 | 0.25±0.09 | 0.11 | 0.26±0.12 | 0.25±0.09 | 0.66 | 0.25±0.1 | 0.26±0.09 | 0.16 |
| SFT (mm) | 26.4±7.7 | 20.9±6.9 | 0.001 | 24.4±8.4 | 20.7±6.8 | 0.003 | 22.6±7.2 | 19.8±6.8 | 0.003 |

HU: Hounsfield unit; L/S: Liver-to-spleen; AST: Aspartate aminotransferase; ALT: Alanine aminotransferase; GGT: Gamma-glutamyl transferase; PLT: Platelet count; FIB-4: Fibrosis-4 ındex; APRI: AST to Platelet ratio ındex; SFT: Subcutaneous fat thickness.

**Table 4.** Results of multiple linear regression analysis for factors associated with the AST/ALT (De Ritis) ratio

| Variable | β (Standardized) | 95% CI | p |
|---|---|---|---|
| Age (years) | -0.07 | -0.28 to 0.14 | 0.49 |
| Male sex | -0.26 | -0.50 to -0.02 | 0.02 |
| Diabetes mellitus | 0.37 | -0.008 to 0.74 | 0.05 |
| Hyperlipidemia | -0.18 | -0.52 to 0.16 | 0.29 |
| GGT (U/L) | -0.40 | -0.52 to -0.27 | <0.001 |
| Liver density (HU) | -0.354 | -2.9 to -1.3 | 0.07 |
| SFT (mm) | 0.08 | -0.18 to 0.36 | 0.51 |

HU: Hounsfield unit; GGT: Gamma-glutamyl transferase; SFT: Subcutaneous fat thickness.

tunistic screening, an optimal cut-off value of ≤58.5 HU was identified, providing a sensitivity of 62.9% and a specificity of 65.3%. Similarly, the liver-spleen attenuation difference and liver-to-spleen ratio showed significant predictive capability (AUC=0.663, p=0.008 and AUC=0.664, p=0.009, respectively). The optimal cut-off for the liver-spleen difference was determined as ≤10.5 HU (sensitivity: 62.9%, specificity: 65.3%), and for the liver-to-spleen ratio as ≤1.23 (sensitivity: 62.9%, specificity: 66.3%). These findings indicate that reduced liver attenuation is significantly associated with elevated GGT levels.

## Discussion

Our study reveals a marked divergence in prevalence rates contingent upon the specific radiological criterion applied. While the use of absolute liver density (<40 HU) limited the identification of steatosis to only 9.3% of the cohort, applying the liver-spleen attenuation difference (<10 HU) significantly broadened the detection rate to 56.8%.

These findings imply that, while absolute density thresholds possess high specificity for moderate-to-severe disease, they may lack the sensitivity required to capture mild forms of steatosis. In the context of early opportunistic screening via unenhanced CT, relative indices such as the L-S difference appear to offer superior diagnostic utility. By utilizing an internal reference, these indices effectively mitigate potential confounders, including inter-scanner variability and fluctuations in patient hematocrit levels. From a technical standpoint, absolute liver attenuation measurements on unenhanced CT are highly susceptible to variations in tube voltage, current, and inter-scanner calibration drifts, even when standardized imaging protocols are employed. Furthermore, systemic patient-related factors, particularly anemia and fluctuations in hematocrit levels, significantly alter blood pool density. Since the liver parenchyma is highly vascular and receives a unique dual blood supply, its absolute Hounsfield unit (HU) values are profoundly influenced by these systemic contrast

**Table 5.** Discriminatory capability of quantitative unenhanced CT parameters for predicting elevated GGT (>50 U/L)

| Parameter | AUC (95% CI) | p | Optimal Cut-off* | Sensitivity (%) | Specificity (%) |
|---|---|---|---|---|---|
| Liver Density (HU) | 0.669 (0.550–0.789) | 0.005 | ≤ 58.5 | 62.9 | 65.3 |
| L-S Difference (HU) | 0.663 (0.541–0.785) | 0.008 | ≤ 10.5 | 62.9 | 65.3 |
| L/S Ratio | 0.664 (0.542–0.785) | 0.009 | ≤ 1.23 | 62.9 | 66.3 |

CT: Computed tomography; AUC: area under the curve; CI: Confidence interval.

alterations. In contrast, the splenic parenchyma possesses a purely arterial supply, and its baseline attenuation remains remarkably stable against acute systemic fluid shifts. By utilizing the spleen as an internal reference standard through the L-S difference, the baseline systemic and technical variability is mathematically canceled out. This leaves a normalized metric that purely reflects changes in the hepatic tissue composition rather than technical artifacts or blood pool attenuation fluctuations, thereby substantially reducing the rate of false-positive or false-negative evaluations in mild steatosis. While our study focused on unenhanced CT, recent advancements suggest that the scope of opportunistic screening is widening. For instance, Derstine et al.[15] utilized artificial intelligence to successfully quantify steatosis on post-contrast scans, suggesting that future metabolic risk assessment need not be limited to non-contrast protocols.

This study shows a relationship between serum GGT levels and diminished liver attenuation. Among the markers analyzed, GGT exhibited the strongest inverse correlation with absolute liver density and emerged as the most predictive variable in ROC analysis. Given GGT's established role as a surrogate for oxidative stress and insulin resistance, this strong radiological-biochemical link reinforces the understanding that hepatic fat accumulation observed on CT represents more than a mere morphological alteration.[11]

It should be noted that the discriminatory performance observed in this study (AUC range: 0.663–0.669) reflects moderate, rather than high, diagnostic accuracy. With sensitivity and specificity values both approximating 63–66%, these quantitative CT thresholds are not intended to function as stand-alone diagnostic tests for elevated GGT or subclinical hepatocellular injury. Rather, their clinical value lies in risk stratification: flagging patients who may benefit from further biochemical evaluation or closer metabolic follow-up during routine, non-hepatic CT reporting. Given the modest AUC values, these thresholds should not replace formal biochemical screening or established non-invasive fibrosis assessment, but instead serve as an adjunctive, opportunistic trigger within a broader diagnostic pathway.

Stratification by radiological thresholds identified the liver-spleen attenuation difference as the most clinically robust metric. Uniquely, this was the only parameter associated with significant elevations across all three liver enzymes (AST, ALT, and GGT) in the steatotic group. These results support the utility of the spleen as an internal control; relative attenuation values appear to align more closely with hepatocellular injury than absolute measurements, which remain vulnerable to technical artifacts.[16] Physiologically, the spleen acts as a metabolic anchor in the setting of metabolic dysfunction-associated steatotic liver disease (MASLD). Unlike the liver, which serves as the primary hub for lipid processing and ectopic fat accumulation, the splenic parenchyma does not undergo fatty infiltration or parenchymal remodeling in response to insulin resistance, systemic inflammation, or dyslipidemia. Therefore, while metabolic stress progressively drives down hepatic HU values through intrahepatocellular lipid deposition, the spleen provides a stable, unaffected baseline. The fact that the L-S difference was the single parameter in our study to show significant correlations across the entire spectrum of hepatic enzymes (AST, ALT, and GGT) underscores this physiological synergy. It indicates that the loss of the normal parenchymal density gradient between the liver and spleen (shifting below 10 HU) is a more sensitive surrogate for active, subclinical hepatocellular injury and oxidative stress than static thresholds of absolute liver density alone.

Our analysis revealed a discordance between non-invasive fibrosis scores: the FIB-4 index significantly correlated with all radiological steatosis parameters, whereas the APRI score did not. This is probably due to the FIB-4 index's composition, which includes an age-related factor strongly linked to metabolic syndrome.[17] This makes it more sensitive in a general population with varying degrees of steatosis. Conversely, APRI is typically more optimized for detecting advanced fibrosis and cirrhosis, which may explain its lack of sensitivity in our predominantly non-cirrhotic cohort.[18,19]

Anthropometric analysis in our study showed that subcutaneous fat thickness (SFT) was consistently and significantly higher in patients with radiologically defined steatosis across all classification methods. This validates the strong link between peripheral adiposity and visceral fat deposition.[20] It suggests that unenhanced CT can serve as a comprehensive tool to assess adiposity, simultaneously visualizing visceral fat and subcutaneous depots, providing a holistic view of the patient's metabolic risk profile.[21]

Collectively, our results demonstrate that quantitative data derived from routine unenhanced CT scans correlate significantly with biochemical markers of liver injury and fibrosis. This supports the paradigm of opportunistic screening. Given that unenhanced chest or abdominal CTs are frequently performed for unrelated clinical indications, radiologists can provide substantial added value by reporting these quantitative metrics, potentially triggering early biochemical workups for undiagnosed metabolic liver disease.[22] It has been shown that FIB-4 and APRI thresholds can effectively rule out cirrhosis even in patients with normal ALT levels.[18] This strengthens the potential value of using such non-invasive models in opportunistic screening cohorts.

The primary strength of this study lies in its comprehensive evaluation of multiple quantitative CT parameters simultaneously against a broad panel of biochemical markers and fibrosis scores. Unlike studies that rely solely on absolute attenuation values, our inclusion of spleen-referenced metrics provides a more robust analysis that mitigates potential scanner-related variability. Furthermore, by incorporating subcutaneous fat thickness (SFT) into the analysis, we were able to demonstrate the link between visceral and peripheral adiposity, reinforcing the utility of unenhanced CT as a holistic tool for metabolic profiling. The use of routine, unenhanced CT data for these calculations highlights the potential for opportunistic screening without incurring additional cost or radiation exposure to the patient.

Our study has several limitations that warrant emphasis. First and foremost, its retrospective, single-center design inherently limits causal inference and may introduce selection bias, while the relatively modest sample size (n=225) constrains the generalizability of the proposed cut-off values to other populations and scanner platforms. Second, the absence of histopathological confirmation via liver biopsy or cross-sectional validation with MRI-proton density fat fraction (MRI-PDFF) represents a fundamental limitation, as it precludes direct validation of the radiological thresholds proposed here against tissue-based or imaging-based ground truth. Consequently, the diagnostic performance metrics reported in this study should be interpreted as associations with biochemical surrogates rather than validated diagnostic accuracy against a true reference standard. Instead, we relied on biochemical surrogates and non-invasive scores (FIB-4, APRI), which, while clinically valid, are indirect markers. Third, due to the retrospective nature of this study, several key confounding variables, including BMI, visceral adiposity (such as visceral fat area [VFA]), baseline hematocrit, and hepatic iron content, were not uniformly available across the entire cohort and could not be integrated into the multivariate regression models. While we utilized subcutaneous fat thickness (SFT) as an accessible and rapidly measurable surrogate for global adiposity during routine abdominal CT reporting, the lack of direct visceral fat quantification restricts our ability to fully differentiate the independent metabolic contributions of visceral versus peripheral fat depots. Furthermore, unmeasured fluctuations in hematocrit or subclinical hepatic iron overload could potentially introduce minor confounding effects on the absolute liver attenuation thresholds. Future prospective investigations with comprehensive anthropometric and laboratory profiling are warranted to control for these systemic variables. Finally, detailed data regarding alcohol consumption and medication history were not available for all patients, which are potential confounding factors in enzymatic analysis.

Future research should focus on validating these quantitative CT thresholds against MRI-proton density fat fraction (MRI-PDFF) or elastography in prospective, multi-center cohorts to establish more precise cut-off values. Longitudinal studies are also warranted to determine whether temporal changes in liver density correlate with dynamic improvements in GGT levels and FIB-4 scores. Additionally, the integration of artificial intelligence algorithms for automated segmentation and measurement of liver and spleen attenuation could standardize this opportunistic screening process. Large-scale population studies have already demonstrated the feasibility of this approach; for instance, Pooler et al.[23] applied fully automated AI-based body composition tools, including hepatic steatosis quantification, across more than 100,000 unenhanced and contrast-enhanced CT examinations performed for unrelated clinical indications. Such automated pipelines, if integrated directly into PACS or radiology reporting workflows, could enable real-time flagging of at-risk patients without added interpretive burden on radiologists, thereby translating opportunistic screening from a research concept into routine clinical practice.

## Conclusion

Unenhanced CT parameters, particularly the liver-spleen attenuation difference and absolute liver density, demonstrate significant predictive potential and strong associations with biochemical markers of metabolic liver injury, such as elevated GGT levels and FIB-4 scores. These findings suggest that accessible quantitative metrics have the potential to serve as complementary opportunistic screening tools to identify patients at risk for MASLD during routine clinical workflows.

### Disclosure

**Ethical Committee Approval:** Approval for this study was obtained from Necmettin Erbakan University Ethics Committee (desicion number: 2025/6199, decision date: 12/12/2025) according to the Helsinki declaration.

**Conflict of Interest:** The authors declare that they have no conflict of interest to declare.

**Funding:** The author declares that this research received no external funding.

**Use of AI for Writing Assistance:** The authors used Google Gemini (Version 3.1 Pro) for text editing and language polishing to improve the readability of the manuscript. The final content was thoroughly reviewed and approved by all human authors, who take full responsibility for the integrity of the work.

**Author Contributions:** Concept – AEA; Design – AEA, HEK; Supervision – HEK; Data Collection and/or Processing – AEA; Analysis and/or Interpretation – HEK; Writing – AEA; Critical Review – HEK.

**Peer-review:** Externally peer-reviewed.

## References


1. Osta EG, Saenz F, Jaganathan S, Thomas C, Tsai E, Surabhi V, Prasad SR, Katabathina VS. Current update on nomenclature, diagnosis, and management of metabolic dysfunction-associated steatotic liver disease: radiologists' perspective. Radiographics 2025;45(12):e240221. [CrossRef]
2. Kalas MA, Chavez L, Leon M, Taweesedt PT, Surani S. Abnormal liver enzymes: A review for clinicians. World J Hepatol 2021;13(11):1688–98. [CrossRef]
3. Gaba RC, Knuttinen MG, Brodsky TR, Palestrant S, Omene BO, Owens CA, Bui JT. Hepatic steatosis: correlations of body mass index, CT fat measurements, and liver density with biopsy results. Diagn Interv Radiol 2012;18(3):282–7. [CrossRef]
4. Chung J, Park HS, Kim YJ, Yu MH, Park S, Jung SI. Association of hepatic steatosis ındex with nonalcoholic fatty liver disease diagnosed by non-enhanced CT in a screening population. Diagnostics (Basel) 2021;11(12):2168. [CrossRef]
5. Graffy PM, Sandfort V, Summers RM, Pickhardt PJ. Automated liver fat quantification at nonenhanced abdominal CT for population-based steatosis assessment. Radiology 2019;293(2):334–42. [CrossRef]
6. Zeb I, Li D, Nasir K, Katz R, Larijani VN, Budoff MJ. Computed tomography scans in the evaluation of fatty liver disease in a population based study: the multi-ethnic study of atherosclerosis. Acad Radiol 2012;19(7):811–8. [CrossRef]
7. Park SH, Kim DJ. Correlation between liver-to-spleen hounsfield unit ratio and metabolic ımprovement in patients with bariatric surgery. J Metab Bariatr Surg 2025;14(1):24–31. [CrossRef]
8. Westfall E, Jeske R, Bader AR. Nonalcoholic fatty liver disease: Common questions and answers on diagnosis and management. Am Fam Physician 2020;102(10):603–12.
9. Sharma P. Value of Liver Function Tests in Cirrhosis. J Clin Exp Hepatol 2022;12(3):948–64. [CrossRef]
10. Luo L, Shao C, Teng L, Zhuo S, Dong Z, Wang W, et al. Liver fibrosis with persistently normal alanine transaminase levels exhibits a distinct treatment response in MASLD. BMJ Open Gastroenterol 2025;12(1):e001895. [CrossRef]
11. Koenig G, Seneff S. Gamma-glutamyltransferase: A predictive biomarker of cellular antioxidant ınadequacy and disease risk. Dis Markers 2015;2015:818570. [CrossRef]
12. Botros M, Sikaris KA. The de ritis ratio: the test of time. Clin Biochem Rev 2013;34(3):117–30.
13. Sterling RK, Lissen E, Clumeck N, Sola R, Correa MC, Montaner J, et al. Development of a simple noninvasive index to predict significant fibrosis in patients with HIV/HCV coinfection. Hepatology 2006; 43: 1317–1325. [CrossRef]
14. Wai CT, Greenson JK, Fontana RJ, Kalbfleisch JD, Marrero JA, Conjeevaram HS, et al. A simple noninvasive index can predict both significant fibrosis and cirrhosis in patients with chronic hepatitis C. Hepatology 2003;38(2):518–26. [CrossRef]
15. Derstine BA, Holcombe SA, Chen VL, Pai MP, Sullivan JA, Wang SC, et al. Quantification of hepatic steatosis on post-contrast computed tomography scans using artificial intelligence tools. Abdom Radiol (NY) 2026;51(2):991–1003. [CrossRef]
16. Kwon JH, Lee SS, Yoon JS, Suk HI, Sung YS, Kim HS, et al. Liver-to-Spleen Volume Ratio Automatically Measured on CT Predicts Decompensation in Patients with B Viral Compensated Cirrhosis. Korean J Radiol 2021;22(12):1985–95. [CrossRef]
17. Dyson JK, McPherson S, Anstee QM. Non-alcoholic fatty liver disease: non-invasive investigation and risk stratification. J Clin Pathol 2013;66(12):1033–45. [CrossRef]
18. Zhang Z, Wang J, Zhu L, Li Y, Zhang S, Pan Y, et al. Optimization of the use of APRI and FIB-4 for ruling out liver cirrhosis in chronic hepatitis B patients with normal alanine aminotransferase. J Viral Hepat 2025;32(2):e14057. [CrossRef]
19. O'Hara G, Mokaya J, Hau JP, Downs LO, McNaughton AL, Karabarinde A, et al. Liver function tests and fibrosis scores in a rural population in Africa: a cross-sectional study to estimate the burden of disease and associated risk factors. BMJ Open 2020;10(3):e032890. [CrossRef]
20. Cucoranu DC, Pop M, Niculescu R, Vunvulea V, Kosovski IB, Togănel RO, et al. Correlation between CT abdominal anthropometric measurements and liver density in ındividuals with non-alcoholic fatty liver disease. Medicina (Kaunas) 2023;59(3):500. [CrossRef]
21. Pickhardt PJ, Jee Y, O'Connor SD, del Rio AM. Visceral adiposity and hepatic steatosis at abdominal CT: association with the metabolic syndrome. AJR Am J Roentgenol 2012;198(5):1100–7. [CrossRef]
22. Li Y, Wang J, Xu G, Si Y, Huang K, Ye Y, et al. Comparison of accuracy of CT parameters across chest, low-dose lung, and abdominal CT in diagnosing steatotic liver disease. BMC Med Imaging 2025;25(1):232. [CrossRef]
23. Pooler BD, Garrett JW, Lee MH, Rush BE, Kuchnia AJ, Summers RM, et al. CT based body composition measures and systemic disease: A population-level analysis using artificial ıntelligence tools in over 100,000 patients. AJR Am J Roentgenol 2025;224(3):e2432216. Erratum in: AJR Am J Roentgenol 2025;224(6):e2533103. [CrossRef]